Excitonic ordering in strongly correlated spin crossover systems: Induced magnetism and excitonic excitation spectrum

Yu. S. Orlov,[1,2,*] S. V. Nikolaev,[1,2] V. I. Kuz'min,[2] A. E. Zarubin,[2] and S. G. Ovchinnikov[1,2]
[1]*Siberian Federal University, Krasnoyarsk, 660041 Russia*
[2]*Kirensky Institute of Physics, Federal Research Center KSC SB RAS, Krasnoyarsk, 660036 Russia*

(Received 4 July 2022; revised 30 September 2022; accepted 2 December 2022; published 13 December 2022)

The effects associated with interatomic hoppings of excitons and the excitonic Bose condensate formation in strongly correlated spin crossover systems are considered in the framework of the effective Hamiltonian for the two-band Kanamori model. The appearance of antiferromagnetic ordering due to the exciton order is found even in the absence of interatomic exchange interaction. The spectrum of excitonic excitations is calculated at various points of the temperature vs crystal field phase diagram. Outside the region of exciton ordering, the spectrum has a gap, which vanishes at the boundary of the exciton condensate phase. The nonuniform spectral weight distribution over the Brillouin zone is found. The role of electron-phonon interaction is discussed as well.

DOI: 10.1103/PhysRevB.106.235120

I. INTRODUCTION

The excitonic condensation and the excitonic insulator state have been under study for a long time, starting with the theoretical papers [1–3]. As shown by Keldysh and Kopaev [3], the modified Bardeen-Cooper-Schrieffer (BCS) theory of superconductivity can be efficiently applied to describe metal-insulator phase transitions in semimetals. The Keldysh-Kopaev model of an excitonic insulator has become the standard method of describing electronic correlations in the weak-interaction limit. In this model the conditions for the excitonic ferromagnetic phase formation has been found [4]. Recently, a new direction in the field of excitonic magnetism had been developed in Mott insulators with a lowest singlet and excited triplet ionic states, the singlet-triplet physics was discussed in the literature in various contents: magnon condensation in quantum dimer models [5–8], bilayer magnets [9], excitons in rare-earth filled skutterudites [10], and spin-state transition in Fe-pnictides [11]. The exchange interaction over an excited triplet term may result in the antiferromagnetic (AFM) interaction and formation of excitonic magnetism [12]. The formation of AFM order in a singlet-triplet model may be considered as the Bose condensation of triplet excitons. The Higgs-mode excitations were identified in the spin-wave dispersion measured in Ca_2RuO_4 by inelasting neutron scattering [13] and in Raman spectra [14].

In Mott insulators with strong spin-orbit coupling (SOC) like $4d$ and $5d$ oxides with t_{2g}^4 configuration, e.g., Re^{3+}, Ru^{4+}, Os^{4+}, Ir^{4+}, the ions in octahedral oxygen coordination have spin $S = 1$ and effective orbital moment $L_{\text{eff}} = 1$. Due to strong SOC the ground state may be stabilized with a singlet total momentum $J = 0$ and a Van Vleck excitation to a triplet state $J = 1$. Thus the Van Vleck magnetism appears in the singlet-triplet physics. There are some other Mott insulator materials where singlet-triplet physics is involved. In rare-earth perovskites $LnCoO_3$ the strong crystal field stabilizes the singlet $S = 0$ state of a Co^{3+} ion. Above this low-spin (LS) state there are an excited intermediate-spin state with $S = 1$ (IS) and a high-spin state with $S = 2$ (HS). Thus a singlet-triplet model is the appropriate model to study excitonic effects. The origin of the excitonic gap is different from the Van Vleck magnetism, nevertheless the properties of both models are rather similar. The two-band Hubbard model is widely used to describe a singlet-triplet physics in $LnCoO_3$ [15–21].

One more example of the singlet-triplet physics is given by spin crossover in $3d$-metal oxides under high pressure (see the review paper [22] and the recent paper on spin crossover in $FeBO_3$ [23]). For oxides with d^5 cations Mn^{2+}, Fe^{3+} both spin states have nonzero spin values, the HS with $S = 5/2$, and the LS with $S = 1/2$, so magnetic properties are expected at all pressures. Contrary, oxides with d^6 cations Fe^{2+}, like FeO and ferropericlase $Fe_xMg_{1-x}O$ ($x = 0.15$–0.20), the LS has $S = 0$ and the HS has $S = 2$. Below critical pressure $P_c = 55$ GPa the HS state is stable, while above P_c the LS nonmagnetic state is realized at room temperature [24–27]. Similar to $LnCoO_3$ such a Mott insulator may be considered within the two-band Hubbard model (with the exception of a few situations when the value of spin $S = 2$ and not $S = 1$ is essential). In our previous paper [28] we have derived the singlet-triplet effective Hamiltonian within a two-band Hubbard-Kanamori model in the regime of strong electronic correlations. This model for two electrons per atom describes two ionic states, the singlet and the triplet, separated by a spin gap which can change its sign by increasing a crystal field parameter. It corresponds to the HS state at low pressure and the LS at high pressure. The electron nearest neighbor hopping results in the AFM exchange interaction between the HS terms, and also in the interatomic hopping of local excitons that has not been studied in Ref. [28]. A mean field phase diagram obtained in Ref. [28] contains the AFM HS phase and nonmagnetic LS phase. The

*jso@iph.krasn.ru

HS exchange interaction results in a shift of the crossover point to higher pressure. The excitonic phase has been found on the border of spin crossover.

Here we have studied the exciton dispersion and have found the formation of the gapless boson spectrum at the boundary of the exciton condensate phase. A peculiar result obtained here is the appearance of AFM excitonic ordering even in the absence of interatomic exchange interaction. The nonuniform excitonic spectral weight over the Brillouin zone is found.

The spin crossover at zero temperature is a quantum phase transition occurring when varying pressure (crystal field). It is characterized by a topological order parameter defined by the geometrical Berry phase, which undergoes a steplike change by 2π at the transition point [29]. Thus, it is of interest to study how quasiparticle (one-particle) and collective excitations change with spin crossover transition. In Ref. [30] we showed that the electronic band structures in the LS and HS states are topologically nonequivalent and cannot be transformed into each other smoothly across a spin crossover transition. We are familiar with Ref. [16], where, within the framework of the effective Hamiltonian obtained from the two-band Hubbard-Kanamori model, the spectrum of collective excitations in the exciton phase was studied in detail—here we study the exciton spectrum outside the ordered phase, but our results qualitatively agree at its border with Ref. [16] and show an appearance of the Goldstone gapless mode when the system enters the exciton condensate phase.

The results presented in this paper are obtained using the X-operator technique for the two-band Hubbard-Kanamori model. For a more detailed understanding of the obtained results, in Sec. V an artificially simplified two-level model of one-electron states interacting with phonons is introduced. It is defined by the Hamiltonian written in analogy with the Hamiltonian of the original problem in the fermion creation/annihilation operators representation. In the framework of such a model, the role of the electron-phonon interaction in formation of the dispersion of excitons and the exciton condensate is discussed. It is found that, contrary to the diagonal electron-phonon interaction, the nondiagonal one leads to the opening of a gap in the excitonic excitation spectrum at the boundary of the excitonic condensate phase.

II. EFFECTIVE HAMILTONIAN

A minimal model of strongly correlated spin crossover systems is the two-band Hubbard-Kanamori model. Its Hamiltonian can be written as

$$H = H_\Delta + H_t + H_{\text{Coulomb}}. \tag{1}$$

Here the first term

$$H_\Delta = \varepsilon_1 \sum_{i,\gamma} c^\dagger_{1i\gamma} c_{1i\gamma} + \varepsilon_2 \sum_{i,\gamma} c^\dagger_{2i\gamma} c_{2i\gamma} \tag{2}$$

contains the one-ion energy of one-particle electron states with the energy levels ε_1 and $\varepsilon_2 = \varepsilon_1 + \Delta$, where Δ is the crystal field energy (for convenience one can assume $\varepsilon_1 = 0$), $c^\dagger_{\lambda i\gamma}$ creates a fermion at orbital $\lambda = 1, 2$, site i, and with spin projection $\gamma = \pm 1/2$. The second term is

$$\begin{aligned} H_t = {} & t_{11} \sum_{\langle i,j\rangle,\gamma} c^\dagger_{1i\gamma} c_{1j\gamma} + t_{22} \sum_{\langle i,j\rangle,\gamma} c^\dagger_{2i\gamma} c_{2j\gamma} \\ & + t_{12} \sum_{\langle i,j\rangle,\gamma} (c^\dagger_{2i\gamma} c_{1j\gamma} + c^\dagger_{1i\gamma} c_{2j\gamma}), \end{aligned} \tag{3}$$

where $t_{\lambda\lambda'}$ is the nearest neighbor hopping parameter. The third term

$$\begin{aligned} H_{\text{Coulomb}} = {} & U \sum_{\lambda,i} c^\dagger_{\lambda i\uparrow} c^\dagger_{\lambda i\downarrow} c_{\lambda i\uparrow} c_{\lambda i\downarrow} + V \sum_{\lambda\neq\lambda',i} c^\dagger_{\lambda i\uparrow} c^\dagger_{\lambda' i\downarrow} c_{\lambda i\uparrow} c_{\lambda' i\downarrow} + V \sum_{\lambda>\lambda',i,\gamma} c^\dagger_{\lambda i\gamma} c^\dagger_{\lambda' i\gamma} c_{\lambda i\gamma} c_{\lambda' i\gamma} \\ & + J_H \sum_{\lambda>\lambda',i,\gamma} c^\dagger_{\lambda i\gamma} c^\dagger_{\lambda' i\gamma} c_{\lambda' i\gamma} c_{\lambda i\gamma} + J_H \sum_{\lambda\neq\lambda',i} c^\dagger_{\lambda i\uparrow} c^\dagger_{\lambda' i\downarrow} c_{\lambda' i\uparrow} c_{\lambda i\downarrow} + J'_H \sum_{\lambda\neq\lambda',i} c^\dagger_{\lambda i\uparrow} c^\dagger_{\lambda i\downarrow} c_{\lambda' i\uparrow} c_{\lambda' i\downarrow} \end{aligned} \tag{4}$$

includes the one-site Coulomb interaction energy. Electron-electron interaction is considered in the Kanamori approximation [31]. It preserves the multiplet character of the electron-electron interaction as much as possible. U is the parameter that describes the direct repulsion between two electrons in the same orbital. V describes the direct repulsion between two electrons in different orbitals. It is assumed that this repulsion is equal between all different orbitals. The process where two electrons are interchanged is described by the exchange integral J_H. The process where two electrons residing in the same orbital scatter on each other and are transferred from one orbital into another is characterized by the integral J'_H.

An important feature of such a two-orbital model is a possibility of formation, at half-filling ($N_e = 2$ is an average number of electrons on a crystal lattice site) and in the zero hopping approximation $t_{\lambda\lambda'} = 0$, of various localized two-electron states with spin values $S = 0, 1$, which makes possible a spin crossover with varying Δ. Within the region $\Delta < \Delta_C = \sqrt{(U - V + J_H)^2 + {J'_H}^2}$ the ground state is the triplet HS state ($S = 1$) $|\sigma\rangle$ with the energy E_{HS}:

$$|\sigma\rangle = \begin{cases} c^\dagger_{1\uparrow} c^\dagger_{2\uparrow} |0\rangle, & \sigma = +1, \\ \frac{1}{\sqrt{2}} (c^\dagger_{1\uparrow} c^\dagger_{2\downarrow} |0\rangle + c^\dagger_{1\downarrow} c^\dagger_{2\uparrow} |0\rangle), & \sigma = 0, \\ c^\dagger_{1\downarrow} c^\dagger_{2\downarrow} |0\rangle, & \sigma = -1, \end{cases}$$

while at $\Delta > \Delta_C$ the ground state is the singlet ($S = 0$) state $|s\rangle = C_1(\Delta) c^\dagger_{1\uparrow} c^\dagger_{1\downarrow} |0\rangle - C_2(\Delta) c^\dagger_{2\uparrow} c^\dagger_{2\downarrow} |0\rangle$ with the energy E_{LS}, where $C_1(\Delta) = \sqrt{1 - C_2^2(\Delta)}$ and $C_2(\Delta) = x/2(1 + x + \sqrt{1 + x})$ are the normalizing coefficients [28] ($x = {J'_H}^2/\Delta^2$).

To obtain an effective Hamiltonian it is convenient to use Hubbard X-operators $X^{p,q} = |p\rangle\langle q|$ [32] built on the eigenstates of the Hamiltonian $H_\Delta + H_{\text{Coulomb}}$:

$$(H_\Delta + H_{\text{Coulomb}})|p\rangle = E_p|p\rangle, \tag{5}$$

with the number of electrons taking values $N_e = 1, 2, 3$. Since the Hubbard operators form a linearly independent basis, any local operator can be represented as a linear combination of the X operators, including the one-electron annihilation operator

$$c_{\lambda i\gamma} = \sum_{pq} |p\rangle\langle p|c_{\lambda i\gamma}|q\rangle\langle q| = \sum_{pq} \chi_{\lambda\gamma}(p,q) X_i^{p,q}. \tag{6}$$

Since the number of eigenstates $|p\rangle$ and $|q\rangle$ is finite, the pairs (p, q) can be numbered by an index m (or n) for convenience [33]. The notation of the diagonal X-operators $X^{p,p}$ remains unchanged.

Using Eq. (6), the anomalous averages $\langle c^\dagger_{2f\gamma} c_{1f\gamma}\rangle$ without and with a spin projection change $\langle c^\dagger_{2f\bar\gamma} c_{1f\gamma}\rangle$ ($\bar\gamma = -\gamma$) can be written as

$$\langle c^\dagger_{2f\gamma} c_{1f\gamma}\rangle \approx -\gamma\sqrt{2}\left(C_2\langle X_f^{s,0}\rangle + C_1\langle X_f^{0,s}\rangle\right), \tag{7}$$

$$\langle c^\dagger_{2f\bar\gamma} c_{1f\gamma}\rangle \approx -2\gamma\left(\gamma + \frac{1}{2}\right)\left(C_2\langle X_f^{s,+1}\rangle + C_1\langle X_f^{+1,s}\rangle\right) + 2\gamma\left(\gamma - \frac{1}{2}\right)\left(C_2\langle X_f^{s,-1}\rangle + C_1\langle X_f^{-1,s}\rangle\right). \tag{8}$$

Here and below, angular brackets denote thermodynamical averages.

As follows from Eqs. (7) and (8), the exciton pairing is described by nonzero averages of singlet-triplet excitations. The Hamiltonian defined by Eq. (1) can be rewritten in the X-operator representation as

$$H = \sum_{i,p} E_p X_i^{p,p} + \sum_{\langle i,j\rangle}\sum_{mn} t^{mn} X_i^{\dagger m} X_j^n, \tag{9}$$

where E_p is the multielectron eigenstate energy and $t^{mn} = \sum_{\lambda,\lambda',\gamma} t_{\lambda\lambda'} \chi^*_{\lambda\gamma}(m)\chi_{\lambda'\gamma}(n)$ is the renormalized hopping integral.

Using the Hamiltonian in Eq. (9) as an initial one, we can obtain an effective Hamiltonian by excluding interband (between the lower and upper Hubbard subbands) hopping in a second order perturbation theory over interatomic electron hopping similar to the t-J model derivation from the Hubbard model. To do this, we apply the projection operator method developed in Ref. [34] for the Hubbard model and in Ref. [35] for the p-d model (see also Refs. [15,16]).

Let us define projection operators P_1 and P_2:

$$P_1 = \left(\sum_\gamma X_i^{1\gamma,1\gamma} + \sum_\gamma X_i^{2\gamma,2\gamma} + X_i^{s,s} + \sum_\sigma X_i^{\sigma,\sigma}\right) \times \left(\sum_\gamma X_j^{1\gamma,1\gamma} + \sum_\gamma X_j^{2\gamma,2\gamma} + X_j^{s,s} + \sum_\sigma X_j^{\sigma,\sigma}\right),$$

where $X_i^{1\gamma,1\gamma}$ and $X_i^{2\gamma,2\gamma}$ are X operators constructed on states of doublets $|1\gamma\rangle = c^\dagger_{1\gamma}|0\rangle$ and $|2\gamma\rangle = c^\dagger_{2\gamma}|0\rangle$ with one electron, respectively. Due to electron-hole symmetry, instead of single-particle states, one can use three-particle states $|1\gamma\rangle = c^\dagger_{1\gamma} c^\dagger_{2\uparrow} c^\dagger_{2\downarrow}|0\rangle$ and $|2\gamma\rangle = c^\dagger_{1\uparrow} c^\dagger_{1\downarrow} c^\dagger_{2\gamma}|0\rangle$. The P_2 operator can be found from the condition of projection operators basis completeness

$$P_2 = 1 - P_1.$$

For P_1 and P_2 the multiply condition is satisfied:

$$P_n P_m = \delta_{mn} P_n.$$

Let us multiply the Hamiltonian in Eq. (9) on the left and on the right by the operators P_n. P_1HP_1 and P_2HP_2 describe processes in the lower and upper Hubbard subbands, respectively. In this case, interband electron hopping are described by the terms P_1HP_2 and P_2HP_1. To exclude interband jumps, we apply the method of operator perturbation theory. Let us represent the Hamiltonian in the form

$$H_\eta = H' + \eta H'',$$

where $H' = P_1HP_1 + P_2HP_2$, $H'' = P_1HP_2 + P_2HP_1$, and η is a formal parameter (we set it equal to one at the end). The essence of this method is that, by applying the canonical transformation

$$H_{\text{eff}} = \exp(-i\eta F) H \exp(i\eta F),$$

we can choose the operator F in such a way that the terms of the Hamiltonian H_{eff}, which are linear in η, i.e., precisely those terms that are responsible for interband hopping, vanish. This requirement leads to the following equation for the F operator:

$$H'' + i[H', F] = 0. \tag{10}$$

Here H_{eff} is defined as

$$H_{\text{eff}} = H_{\text{eff}}(\eta = 1) = H' + \tfrac{1}{2} i[H'', F]. \tag{11}$$

Omitting the solution (10) and (11) given in Ref. [34], as a result, we obtain

$$H_{\text{eff}} = P_1HP_1 + P_2HP_2 - \frac{1}{\Omega_g}[P_1HP_2, P_2HP_1],$$

where Ω_g is the energy interval between the centers of the upper and lower Hubbard subbands (charge-transfer energy).

The obtained effective Hamiltonian is

$$H_{\text{eff}} = H_S + H_{nn} + H_{\text{ex}}. \tag{12}$$

Here the first term describes an AFM exchange contribution to the Heisenberg-like Hamiltonian

$$H_S = \frac{1}{2} J \sum_{\langle i,j\rangle}\left(\mathbf{S}_i\mathbf{S}_j - \frac{1}{4} n_i n_j\right), \tag{13}$$

where $\mathbf{S}_i$ is the $S = 1$ spin operator: $S_i^+ = \sqrt{2}(X_i^{+1,0} + X_i^{0,-1})$, $S_i^- = \sqrt{2}(X_i^{0,+1} + X_i^{-1,0})$, and $S_i^z = X_i^{+1,+1} + X_i^{-1,-1}$ [36]; $J = (t_{11}^2 + 2t_{12}^2 + t_{22}^2)/\Omega_g$ is the interatomic exchange interaction; $n_i = 2(X_i^{s,s} + \sum_\sigma X_i^{\sigma,\sigma}) = 2(n_i^{\text{LS}} + n_i^{\text{HS}})$ is the particle number operator at site i [$n_i^{\text{LS(HS)}}$ is the occupation operator of the LS (HS) state]. Using the completeness condition $X^{s,s} + \sum_\sigma X^{\sigma,\sigma} = 1$, one can show that $\langle n_i\rangle = 2(\langle n_i^{\text{LS}}\rangle + \langle n_i^{\text{HS}}\rangle) = 2(n_{\text{LS}} + n_{\text{HS}}) = 2$.

The next term

$$H_{nn} = \frac{1}{2}\tilde{J}\sum_{\langle i,j\rangle} X_i^{s,s}X_j^{s,s}, \tag{14}$$

where $\tilde{J} = [1-(2C_1C_2)^2](t_{11}^2 - 2t_{12}^2 + t_{22}^2)/\Omega_g$, represents a density-density type interaction of LS states.

The third term in Eq. (12),

$$H_{\rm ex} = -\frac{\varepsilon_S}{2}\sum_i\left(X_i^{s,s} - \sum_{\sigma=-S}^{+S} X_i^{\sigma,\sigma}\right) + \sum_\sigma\sum_{\langle i,j\rangle} \times\left[\frac{1}{2}J'_{\rm ex}\left(X_i^{\sigma,s}X_j^{s,\sigma} + X_i^{s,\sigma}X_j^{\sigma,s}\right) - \frac{1}{2}J''_{\rm ex}(-1)^{|\sigma|} \times\left(X_i^{\sigma,s}X_j^{\bar{\sigma},s} + X_i^{s,\sigma}X_j^{s,\bar{\sigma}}\right)\right], \tag{15}$$

contains singlet and triplet energies as well as interatomic hoppings of excitons with the amplitude $J'_{\rm ex}$ as well as creation/annihilation processes of biexcitons on neighboring sites with the amplitude $J''_{\rm ex}$. In the absence of any cooperative interactions, at negative values of the spin gap $\varepsilon_S = E_{\rm HS} - E_{\rm LS}$ the ground state is the HS state, whereas at positive spin gap values, the ground state is the LS state; $J'_{\rm ex} = 2C_1C_2(t_{11}t_{22} - t_{12}^2)/\Omega_g$, $J''_{\rm ex} = (t_{11}t_{22} - t_{12}^2)/\Omega_g$, $\bar{\sigma} = -\sigma$. The Hubbard operators $X_i^{\bar{\sigma},s}$ and $X_i^{s,\sigma}$ in Eq. (15) describe Bose-like excitations (excitons) between the LS singlet state $|s\rangle$ and the HS triplet state $|\sigma\rangle$. The first term within the square brackets in Eq. (15) describes the excitonic dispersion by means of interatomic hoppings (such a dispersion was considered long ago in the work of Vonsovskii and Svirskii [37]). The second term in Eq. (15) contains creation/annihilation processes of biexcitons at neighboring sites of a lattice, which makes the dispersion more complicated compared to the usual one obtained within the tight-binding method [37]. Near the spin crossover, the normalization constants defined above take values $C_1 \approx 1$ and $C_2 \approx 0$, thus, $J'_{\rm ex} \approx 0$ [28]. At such circumstances, the biexciton excitations play the main role in the formation of the excitonic dispersion.

III. PHASE DIAGRAMS IN THE MEAN FIELD APPROXIMATION

In the mean field approximation (MF) for two AFM sublattices A and B, the terms in Eqs. (13)–(15) can be expressed as the following Eqs. (16)–(18):

$$H_S^{\rm MF} = zJm_B\sum_{i_A} S_{i_A}^z + zJm_A\sum_{i_B} S_{i_B}^z - zJ\frac{1}{4}n_B\sum_{i_A} n_{i_A} - zJ\frac{1}{4}n_A\sum_{i_B} n_{i_B} - \frac{1}{2}zJNm_Am_B + \frac{1}{2}zJN, \tag{16}$$

where z is a number of nearest neighbors and $m_{A(B)} = \langle S_{i_{A(B)}}^z\rangle$ is an $A(B)$-sublattice magnetization;

$$H_{nn}^{\rm MF} = z\tilde{J}n_{{\rm LS},B}\sum_{i_A} n_{i_A}^{LS} + z\tilde{J}n_{{\rm LS},A}\sum_{i_B} n_{i_B}^{\rm LS} - z\tilde{J}\frac{N}{2}n_{{\rm LS},A}n_{{\rm LS},B}. \tag{17}$$

The interaction proportional to $\tilde{J}$ leads to an additional cooperation mechanism, but in the following we will mainly neglect it to simplify the results, since it does not influence the behavior of phase diagrams qualitatively, leading only to the sublattices LS energies renormalization:

$$H_{\rm ex}^{\rm MF} = \sum_F\sum_{\sigma=\pm1,0}\left\{zJ'_{\rm ex}\Delta_{{\rm ex},\bar{F}}^\sigma\sum_{i_F}\left(X_{i_F}^{s,\sigma} + X_{i_F}^{\sigma,s}\right) - (-1)^{|\sigma|}zJ''_{\rm ex}\Delta_{{\rm ex},\bar{F}}^\sigma\sum_{i_F}\left(X_{i_F}^{s,\bar{\sigma}} + X_{i_F}^{\bar{\sigma},s}\right) - \frac{1}{2}zN\left(J'_{\rm ex}\Delta_{{\rm ex},F}^\sigma\Delta_{{\rm ex},\bar{F}}^\sigma - (-1)^{|\sigma|}J''_{\rm ex}\Delta_{{\rm ex},F}^\sigma\Delta_{{\rm ex},\bar{F}}^{\bar{\sigma}}\right)\right\} - \varepsilon_S\sum_{i_A} X_{i_A}^{s,s} - \varepsilon_S\sum_{i_B} X_{i_B}^{s,s} + N\frac{\varepsilon_S}{2}, \tag{18}$$

where $F = (A,B)$ ($\bar{F} = A$ if $F = B$ and vice versa), $\Delta_{{\rm ex},A(B)}^\sigma = \langle X_{i_A(i_B)}^{s,\sigma}\rangle$ are the excitonic order parameter components, which satisfy the equation $(\Delta_{\rm ex}^\sigma)^\dagger = \langle X^{\sigma,s}\rangle = \Delta_{\rm ex}^\sigma$ at thermodynamic equilibrium. Note that, when $\Delta_{\rm ex}^\sigma \neq 0$, a quantum mechanical mixture of the LS and HS states is present, albeit in the absence of spin-orbital interaction.

By solving the eigenstate problem

$$H_{\rm eff}^{\rm MF}|\psi\rangle_k = E_k|\psi\rangle_k, \tag{19}$$

where $|\psi\rangle_k = C_{{\rm LS},k}|s\rangle + \sum_\sigma C_{{\rm HS},k}|\sigma\rangle$ are the eigenstates of the Hamiltonian $H_{\rm eff}^{\rm MF} = H_S^{\rm MF} + H_{nn}^{\rm MF} + H_{\rm ex}^{\rm MF}$, and using the roots corresponding to the minimum of the free energy $F = -k_BT\ln Z$, where $Z = \sum_k e^{-E_k/k_BT}$ is the partition function, various thermodynamic averages included in $H_{\rm eff}^{\rm MF}$ can be calculated:

$$\Delta_{{\rm ex},A(B)}^\sigma = \sum_k\frac{\langle\psi_k|X_{i_A(i_B)}^{s,\sigma}|\psi_k\rangle e^{-E_k/k_BT}}{Z},$$

$$m_{A(B)} = \sum_k\frac{\langle\psi_k|S_{i_{A(B)}}^z|\psi_k\rangle e^{-E_k/k_BT}}{Z},$$

$$n_{{\rm HS},A(B)} = \sum_k\frac{\langle\psi_k|\sum_\sigma X_i^{\sigma,\sigma}|\psi_k\rangle e^{-E_k/k_BT}}{Z}.$$

Thus, when solving Eq. (19), one deals with a self-consistent problem of finding the eigenstates and the eigenvalues of the effective Hamiltonian in the mean field approximation. Figures 1 and 2 show the dependence of the excitonic order parameter components $\Delta_{\rm ex}^\sigma$, the HS state occupation $n_{\rm HS}$, and

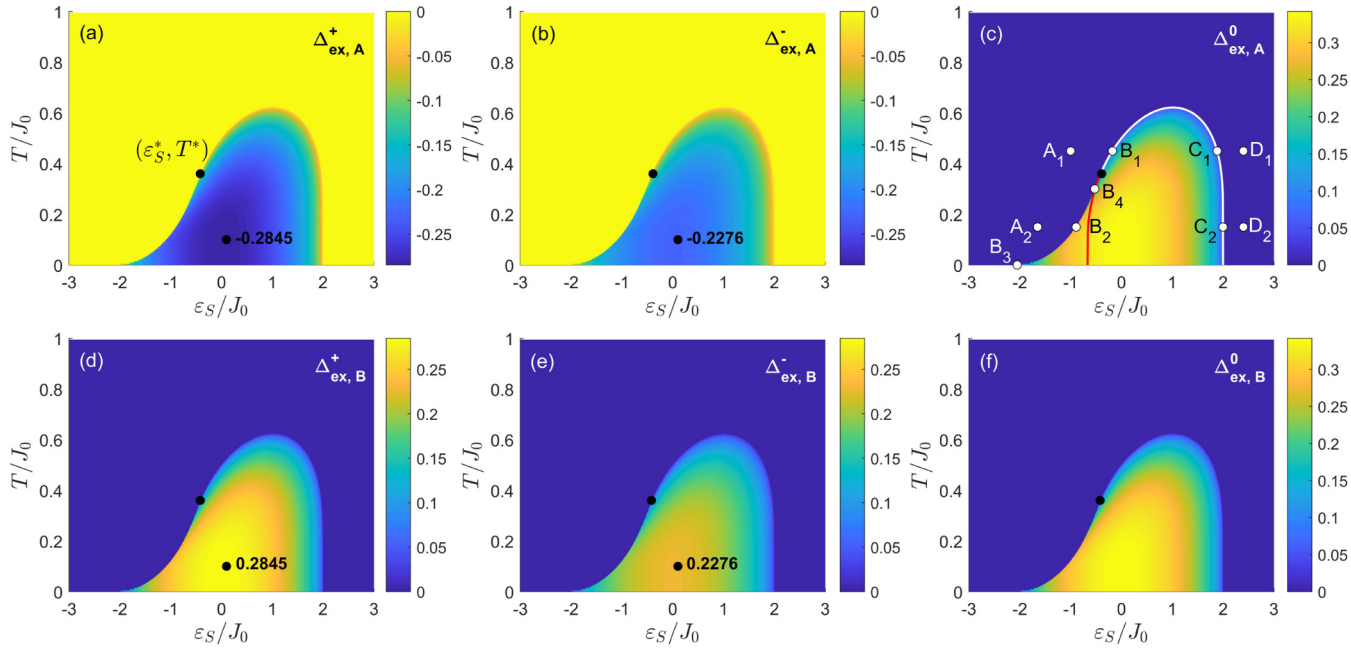

FIG. 1. The calculated phase diagrams of the excitonic order parameter components Δ^{σ}_{ex} for the sublattices A and B at zero value of the interatomic exchange interaction J; the parameters are $z = 4$, $J''_{ex} = 0.5J_0$, $J_0 = 28$ K; (ε_S^*, T^*) is the tricritical point. The values of $\Delta^{\sigma}_{ex,A(B)}$ at the point $(\varepsilon_S/J_0 = 0.1, T/J_0 = 0.1)$ on (a), (b) and (d), (e) are shown for example. Here and below at points A, B, C, D in (c) the excitonic spectrum is calculated. The white line shows the boundary of the second order phase transition. The red curve indicates the right boundary of the metastable state region.

magnetization m for the two sublattices A and B on temperature T and spin gap (crystal field) ε_S. The calculations were done omitting the interatomic exchange ($J = 0$). However, to compare conveniently with the $J \neq 0$ case [28], T and ε_S are shown in units of the exchange integral $J = J_0 = 28$ K [38]; $z = 4$, $J''_{ex} = 0.5J_0$. From Figs. 2(a) and 2(c) it is seen that $n_{HS,A} = n_{HS,B}$; $m_A = -m_B$, so the long-range antiferromagnetic ordering is realized [Figs. 2(b) and 2(d)] even at $J = 0$, since $\Delta^{+}_{ex,A(B)} \neq \Delta^{-}_{ex,A(B)}$ [Figs. 1(a) and 1(b) and Figs. 1(d) and 1(e)], $\Delta^{0}_{ex,A} = \Delta^{0}_{ex,B}$ [Figs. 1(c) and 1(f)], and $\Delta^{+/-}_{ex,A} = -\Delta^{+/-}_{ex,B}$; for example, in Fig. 1 the values of $\Delta^{\sigma}_{ex,A(B)}$ at the point $(\varepsilon_S/J_0 = 0.1, T/J_0 = 0.1)$ are shown.

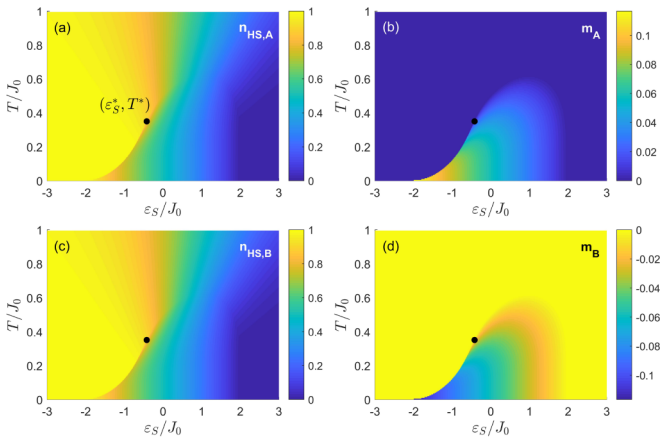

FIG. 2. The phase diagrams of (a) and (c) the HS state occupation and (b) and (d) magnetization for both sublattices demonstrating the AFM order without interatomic exchange interaction; (ε_S^*, T^*) is the tricritical point.

The phase diagrams in Figs. 1 and 2 clearly show an existence of a special point, which is the tricritical point (T^*, ε_S^*), where the line of the second order phase transitions smoothly transforms into the line of first order phase transitions. In the region $\varepsilon_S > \varepsilon_S^*$ [see Figs. 2(b) and 2(d)] the system undergoes a second order phase transition from an antiferromagnetic (HS) state to a paramagnetic state with rising temperature; contrarily, at $\varepsilon_S < \varepsilon_S^*$ there is a first order phase transition.

We note that all the presented phase diagrams are asymmetrical with respect to the change of the sign of the spin gap. Contrarily, the toy model considered below in Sec. V possesses such a symmetry. The difference in the multielectron terms (the phase diagrams in Figs. 1 and 2 are obtained using the two-electron singlet and triplet terms) is related to the different degeneracy multiplicity of the HS and LS states, which leads to a broken symmetry with respect to the spin gap sign inversion.

IV. SPECTRUM OF EXCITONS

Let us consider the two-particle Green functions at finite temperatures in terms of the initial fermion operators to describe collective (in terms of the electron system) excitonic excitations without a spin projection change

$$\mathbf{G}_{(2)} = \begin{pmatrix} \left\langle\left\langle c^{\dagger}_{1f\gamma} c_{2f\gamma} \,\middle|\, c^{\dagger}_{2g\gamma} c_{1g\gamma} \right\rangle\right\rangle_{\omega} & \left\langle\left\langle c^{\dagger}_{1f\gamma} c_{2f\gamma} \,\middle|\, c^{\dagger}_{1g\gamma} c_{2g\gamma} \right\rangle\right\rangle_{\omega} \\ \left\langle\left\langle c^{\dagger}_{2f\gamma} c_{1f\gamma} \,\middle|\, c^{\dagger}_{2g\gamma} c_{1g\gamma} \right\rangle\right\rangle_{\omega} & \left\langle\left\langle c^{\dagger}_{2f\gamma} c_{1f\gamma} \,\middle|\, c^{\dagger}_{1g\gamma} c_{2g\gamma} \right\rangle\right\rangle_{\omega} \end{pmatrix} \tag{20}$$

and with a spin projection change

$$\bar{\mathbf{G}}^{\pm}_{(2)} = \begin{pmatrix} \left\langle\!\left\langle c^{\dagger}_{1f\gamma}c_{2f\bar{\gamma}} \;\middle|\; c^{\dagger}_{2g\bar{\gamma}}c_{1g\gamma}\right\rangle\!\right\rangle_{\omega} & \left\langle\!\left\langle c^{\dagger}_{1f\gamma}c_{2f\bar{\gamma}} \;\middle|\; c^{\dagger}_{1g\bar{\gamma}}c_{2g\gamma}\right\rangle\!\right\rangle_{\omega} \\ \left\langle\!\left\langle c^{\dagger}_{2f\gamma}c_{1f\bar{\gamma}} \;\middle|\; c^{\dagger}_{2g\bar{\gamma}}c_{1g\gamma}\right\rangle\!\right\rangle_{\omega} & \left\langle\!\left\langle c^{\dagger}_{2f\gamma}c_{1f\bar{\gamma}} \;\middle|\; c^{\dagger}_{1g\bar{\gamma}}c_{2g\gamma}\right\rangle\!\right\rangle_{\omega} \end{pmatrix}. \tag{21}$$

Using Eq. (6), one can write Eqs. (20) and (21) as

$$\mathbf{G}_{(2)} \approx \frac{1}{2}\left(C_2^2 - C_1^2\right)\begin{pmatrix} G^0_{fg}(\omega) & -L^0_{fg}(\omega) \\ L^0_{fg}(\omega) & -G^0_{fg}(\omega) \end{pmatrix} \tag{22}$$

and

$$\bar{\mathbf{G}}^{\pm}_{(2)} \approx \left(C_1^2 - C_2^2\right)\begin{pmatrix} G^{\pm}_{fg}(\omega) & -L^{\pm}_{fg}(\omega) \\ L^{\pm}_{fg}(\omega) & -G^{\pm}_{fg}(\omega) \end{pmatrix}, \tag{23}$$

where

$$G^{\sigma}_{fg}(\omega) = \left\langle\!\left\langle X^{s,\sigma}_{f} \;\middle|\; X^{\sigma,s}_{g}\right\rangle\!\right\rangle_{\omega}, \tag{24}$$

$$L^{\sigma}_{fg}(\omega) = \left\langle\!\left\langle X^{\bar{\sigma},s}_{f} \;\middle|\; X^{\sigma,s}_{g}\right\rangle\!\right\rangle_{\omega}. \tag{25}$$

The "+(−)" sign in Eq. (23) corresponds to the $\gamma = \uparrow$ ($\downarrow$) spin projection in Eq. (21).

Within Hubbard-1 approximation $\langle X_f^{\sigma' \neq \sigma,\sigma}\rangle = 0$. In the two-sublattice case one obtains

$$G^{\sigma}_{AA,\mathbf{k}}(\omega) = F_{A,\sigma}\big[-J'_{ex}(\mathbf{k})G^{\sigma}_{AB,\mathbf{k}}(\omega) + (-1)^{|\sigma|}J''_{\mathrm{ex}}(\mathbf{k})L^{\sigma}_{AB,\mathbf{k}}(\omega) - 1\big]/(\omega - \varepsilon_B), \tag{26}$$

$$G^{\sigma}_{AB,\mathbf{k}}(\omega) = F_{B,\sigma}\big[-J'_{\mathrm{ex}}(\mathbf{k})G^{\sigma}_{AA,\mathbf{k}}(\omega) + (-1)^{|\sigma|}J''_{\mathrm{ex}}(\mathbf{k})L^{\sigma}_{AA,\mathbf{k}}(\omega)\big]/(\omega - \varepsilon_A), \tag{27}$$

$$L^{\sigma}_{AA,\mathbf{k}}(\omega) = F_{A,\sigma}\big[J'_{ex}(\mathbf{k})L^{\sigma}_{AB,\mathbf{k}}(\omega) - (-1)^{|\sigma|}J''_{\mathrm{ex}}(\mathbf{k})G^{\sigma}_{AB,\mathbf{k}}(\omega)\big]/(\omega + \varepsilon_B), \tag{28}$$

$$L^{\sigma}_{AB,\mathbf{k}}(\omega) = F_{B,\sigma}\big[J'_{\mathrm{ex}}(\mathbf{k})L^{\sigma}_{AA,\mathbf{k}}(\omega) - (-1)^{|\sigma|}J''_{\mathrm{ex}}(\mathbf{k})G^{\sigma}_{AA,\mathbf{k}}(\omega)\big]/(\omega + \varepsilon_A), \tag{29}$$

where $\varepsilon_{A(B)} = \varepsilon_S + \sigma\frac{1}{2}zJm_{A(B)}$, $F_{A(B),\sigma} = \langle X^{\sigma,\sigma}_{A(B)}\rangle - \langle X^{s,s}_{A(B)}\rangle$; $J'_{\mathrm{ex}}(\mathbf{k})$ and $J''_{\mathrm{ex}}(\mathbf{k})$ are the Fourier transforms of J'_{ex} and J''_{ex}. Within the region of the exciton ordering, the occupation numbers and the factors $F_{A(B),\sigma}$ depend on projection σ and sublattice numbers. Thus, magnetization is induced even at $J = 0$, as it is shown in Figs. 2(b) and 2(d).

From Eqs. (26)–(29), the following excitonic spectrum can be obtained:

$$\omega^2_{\mathbf{k},\sigma} = \varepsilon_S^2 + F_{A,\sigma}F_{B,\sigma}\left(J'^{\,2}_{\mathrm{ex}}(\mathbf{k}) - J''^{\,2}_{ex}(\mathbf{k})\right) \pm 2J'_{\mathrm{ex}}(\mathbf{k})\varepsilon_S\sqrt{F_{A,\sigma}F_{B,\sigma}}. \tag{30}$$

The excitonic order parameter does not appear explicitly in Eqs. (26)–(29) defining the Green functions. However, it is related to the occupation numbers $\langle X^{\sigma,\sigma}_{A(B)}\rangle$ and $\langle X^{s,s}_{A(B)}\rangle$ calculated within the self-consistent problem given by Eq. (19). Outside the excitonic region (when $\Delta^{\sigma}_{ex,A(B)} = 0$), one has

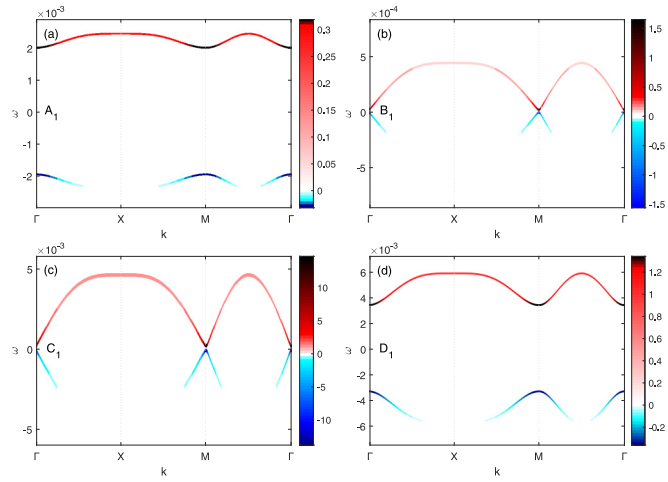

FIG. 3. The excitonic spectrum $\omega^{\pm}_{\mathbf{k},\sigma}$ defined by Eq. (31) at the points A_1, B_1, C_1, and D_1 (along the $T/J_0 = 0.45$ line) of the phase diagram in Fig. 1(c). Here and below the color is proportional to the spectral weight of the excitations.

$F_{A(B),\sigma} = F$ [see Figs. 1(c) and 1(f)]. This way, at $J = 0$, instead of Eq. (30), one can use the expression

$$\omega^{\pm}_{\mathbf{k},\sigma} = \pm\sqrt{(\varepsilon_S - FJ'_{\mathrm{ex}}(\mathbf{k}))^2 - F^2J''^{\,2}_{\mathrm{ex}}(\mathbf{k})}. \tag{31}$$

In Figs. 3–5 the spectrum $\omega^{\pm}_{\mathbf{k},\sigma}$ calculated at different points labeled as A, B, C, and D in Fig. 1(c) is drawn in the case of a two-dimensional (2D) square lattice within the paramagnetic Brillouin zone. Here and below $\Gamma(0,0)$, $X(\pi,0)$, and $M(\pi,\pi)$ are the high-symmetry points. In Fig. 1(c), the white (before the tricritical point) and red (after the tricritical point) lines mark the boundary of the region within which the spectrum defined by Eq. (30) becomes complex, which means that the normal state of the system is unstable with respect to the formation of the excitonic condensate. The white curve strictly coincides with the second order phase transition line. The red curve indicates what the boundary of the normal

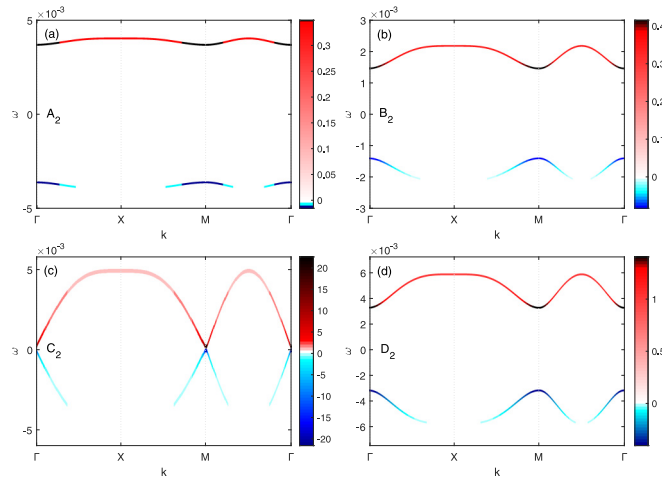

FIG. 4. The excitonic spectrum $\omega^{\pm}_{\mathbf{k},\sigma}$ defined by Eq. (31) at the points A_2, B_2, C_2, and D_2 (along the $T/J_0 = 0.15$ line) of the phase diagram in Fig. 1(c).

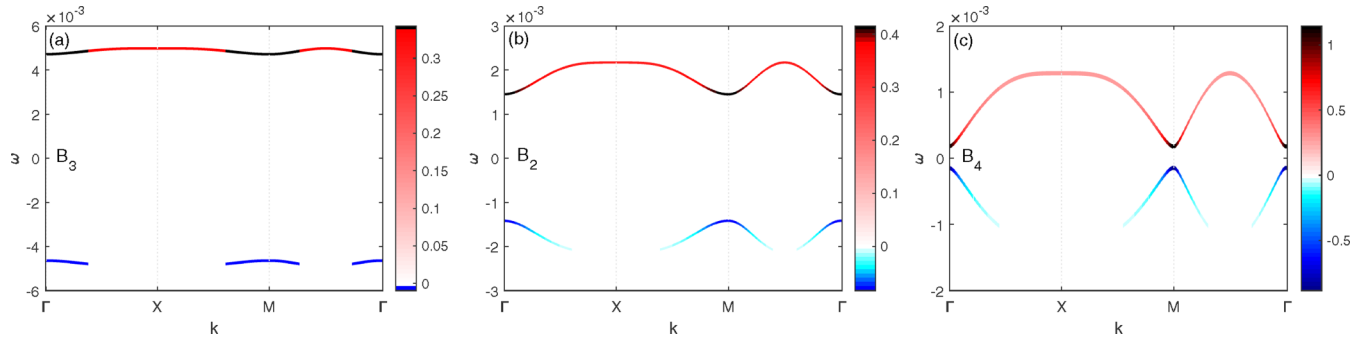

FIG. 5. The excitonic spectrum $\omega^{\pm}_{\mathbf{k},\sigma}$ defined by Eq. (31) at the points B_3, B_2, and B_4, (along the boundary of the second order phase transition) of the phase diagram in Fig. 1(c).

state instability would look like if the region of the first order phase transition did not exist. However, in our calculations, this curve enters the excitonic region right after the tricritical point (ε^*_S, T^*) and strictly coincides with the right boundary of the metastable state region, which always exists in the case of a first order phase transition.

The upper band has a positive spectral weight, which points at "quasiparticle" excitations, whereas the lower band is of a "hole" type and has negative spectral weight (Figs. 3–5). When these bands merge at $\omega = 0$, a transition to a new state associated with the formation of the excitonic condensate occurs—the whole spectral weight concentrates at the points Γ and M (Figs. 3–5). The spectral weight is distributed nonuniformly among the Brillouin zone. Particularly, it is suppressed around the points $(\pi, 0)$ and $(\pi/2, \pi/2)$ in the lower band at any value of ε_S. Concerning the Fermi-type quasiparticle excitations, their unusual spectral weight distribution (inversion) due to topological properties of spin crossover was discussed in our work [30], where the electronic band structure of the strongly correlated spin crossover systems was considered both in the LS and HS states.

Figure 5 shows that the gap in the spectrum remains nonzero throughout the first order phase transition line, and the value of the gap decreases while approaching the tricritical point, at which it vanishes.

V. TOY MODEL

The Hamiltonian in Eq. (18) has a significantly complex phase diagram and a multicomponent excitonic order parameter. Let us try to simplify as much as possible the case considered above and analyze the influence of electron-phonon interaction at the formation of excitonic condensate using an example of an artificially simplified Hamiltonian of a two-level system with local one-electron states "1" and "2" with the energies ε_1 and ε_2 $(\varepsilon = \varepsilon_2 - \varepsilon_1)$ without strong electron correlations. Instead of Eq. (15) we will now use the analogous in essence Eq. (32) in terms of one-particle fermionic operators $c_{\lambda i\gamma}$ $(c^{\dagger}_{\lambda i\gamma})$ of annihilation (creation) of electrons at site i, state $\lambda = 1, 2$ with spin projection $\gamma = \pm 1/2$:

$$\hat{H}_{\rm ex} = \varepsilon_1 \sum_{i,\gamma} c^{\dagger}_{1i\gamma} c_{1i\gamma} + \varepsilon_2 \sum_{i,\gamma} c^{\dagger}_{2i\gamma} c_{2i\gamma} + \frac{J'_1}{2} \sum_{\langle i,j\rangle,\gamma} (c^{\dagger}_{1i\gamma} c_{2i\gamma} c^{\dagger}_{2j\gamma} c_{1j\gamma} + \text{H.c.}) + \frac{J'_2}{2} \sum_{\langle i,j\rangle,\gamma} (c^{\dagger}_{1i\gamma} c_{2i\bar{\gamma}} c^{\dagger}_{2j\bar{\gamma}} c_{1j\gamma} + \text{H.c.})$$
$$+ \frac{J''_1}{2} \sum_{\langle i,j\rangle,\gamma} (c^{\dagger}_{2i\gamma} c_{1i\gamma} c^{\dagger}_{2j\gamma} c_{1j\gamma} + \text{H.c.}) + \frac{J''_2}{2} \sum_{\langle i,j\rangle,\gamma} (c^{\dagger}_{2i\gamma} c_{1i\bar{\gamma}} c^{\dagger}_{2j\bar{\gamma}} c_{1j\gamma} + \text{H.c.}). \tag{32}$$

For example, whereas in Eq. (15) the operator $X^{\sigma,s}_i$ describes a transition from the two-particle singlet state $|s\rangle$ to the triplet state $|\sigma\rangle$, an analogous role in Eq. (32) is played by the operator structure $c^{\dagger}_{2j\gamma} c_{1j\gamma}$ (without a change of a spin projection) or $c^{\dagger}_{2j\bar{\gamma}} c_{1j\gamma}$ (with a change of spin projection). Below we will drop the latter: $J'_2 = J''_2 = 0$, so $J'_1 = J'_{\rm ex}$ and $J''_1 = J''_{\rm ex}$.

Taking into account the electron-phonon interaction, one has

$$H = H_{\rm ex} + H_{\rm 1ph} + H_{\rm 2ph}, \tag{33}$$

where

$$H_{\rm 1ph} = \hbar\omega_{0(1)} \sum_i \left(a^{\dagger}_i a_i + \frac{1}{2}\right) - \frac{1}{2} V_a \sum_{\langle i,j\rangle} (a_i + a^{\dagger}_i)(a_j + a^{\dagger}_j)$$
$$+ g_1 \sum_{i,\gamma} (a_i + a^{\dagger}_i)(c^{\dagger}_{1i\gamma} c_{1i\gamma} - c^{\dagger}_{2i\gamma} c_{2i\gamma}), \tag{34}$$
$$H_{\rm 2ph} = \hbar\omega_{0(2)} \sum_i \left(b^{\dagger}_i b_i + \frac{1}{2}\right) - \frac{1}{2} V_b \sum_{\langle i,j\rangle} (b_i + b^{\dagger}_i)(b_j + b^{\dagger}_j)$$
$$+ g_2 \sum_{i,\gamma} (b_i + b^{\dagger}_i)(c^{\dagger}_{2i\gamma} c_{1i\gamma} + c^{\dagger}_{1i\gamma} c_{2i\gamma}). \tag{35}$$

The term in Eq. (34) contains the diagonal electron-phonon interaction. Next, the term in Eq. (35) describes off-diagonal electron-phonon transition processes between the states 1 and 2. Here $g_{1(2)}$ are the constants of electron-phonon interaction, $\omega_{0(1,2)}$ are the frequencies of a- and b-type phonons. The terms proportional to $V_{a(b)}$ describe interactions of a (b) phonons at different sites of a crystal lattice.

Within the mean field approximation applied to the matrix Green function

$$\mathbf{G}^{\gamma}(\omega) = \begin{pmatrix} \langle\langle c_{1f\gamma} \mid c^{\dagger}_{1g\gamma}\rangle\rangle & \langle\langle c_{1f\gamma} \mid c^{\dagger}_{2g\gamma}\rangle\rangle \\ \langle\langle c_{2f\gamma} \mid c^{\dagger}_{1g\gamma}\rangle\rangle & \langle\langle c_{2f\gamma} \mid c^{\dagger}_{2g\gamma}\rangle\rangle \end{pmatrix}_{\omega} = \begin{pmatrix} G^{\gamma}_{11} & G^{\gamma}_{12} \\ G^{\gamma}_{21} & G^{\gamma}_{22} \end{pmatrix}_{\omega} \tag{36}$$

one has

$$G^{\gamma}_{11(22)}(\omega) = \frac{\omega \mp \frac{\varepsilon}{2} \pm g_1\Delta_{1\mathrm{ph}}}{(\omega-\omega_1)(\omega-\omega_2)},$$

$$G^{\gamma}_{12}(\omega) = G^{\gamma}_{21}(\omega) = \frac{\left(zJ_{\mathrm{ex}}\Delta_{\mathrm{ex}} + g_2\Delta_{2\mathrm{ph}}\right)}{(\omega-\omega_1)(\omega-\omega_2)},$$

where $J_{\mathrm{ex}} = J'_{\mathrm{ex}} + J''_{\mathrm{ex}}$, $\Delta_{1\mathrm{ph}} = \langle a_i + a_i^{\dagger}\rangle$, $\Delta_{2\mathrm{ph}} = \langle b_i + b_i^{\dagger}\rangle$, $\Delta_{\mathrm{ex}} = \langle c^{\dagger}_{2j\gamma}c_{1j\gamma}\rangle = \langle c^{\dagger}_{1j\gamma}c_{2j\gamma}\rangle$ is the excitonic order parameter, and the dispersion is

$$\omega_{1(2)} = \pm\left[\left(\frac{\varepsilon}{2} - g_1\Delta_{1\mathrm{ph}}\right)^2 + \left(zJ_{\mathrm{ex}}\Delta_{\mathrm{ex}} + g_2\Delta_{2\mathrm{ph}}\right)^2\right]^{1/2} = \pm s. \tag{37}$$

In terms of the Matsubara frequencies ω_n and ε_n, and using the mean field approximation with respect to the phonon-phonon interaction $V_{a(b)}$ in Eqs. (34) and (35) one obtains

$$\Delta_{1\mathrm{ph}} = \langle a_i + a_i^{\dagger}\rangle_{\omega_n=0} = \frac{2g_1}{(\hbar\omega_{0(1)} - 2zV_a)} \times \frac{1}{\beta}\sum_{m,\gamma}[\langle c^{\dagger}_{2i\gamma}c_{2i\gamma}\rangle_{\varepsilon_m} - \langle c^{\dagger}_{1i\gamma}c_{1i\gamma}\rangle_{\varepsilon_m}], \tag{38}$$

$$\Delta_{2\mathrm{ph}} \equiv \langle b_i + b_i^{\dagger}\rangle_{\omega_n=0} = -\frac{2g_2}{(\hbar\omega_{0(2)} - 2zV_b)} \times \frac{1}{\beta}\sum_{m,\gamma}[\langle c^{\dagger}_{1i\gamma}c_{2i\gamma}\rangle_{\varepsilon_m} + \langle c^{\dagger}_{2i\gamma}c_{1i\gamma}\rangle_{\varepsilon_m}]. \tag{39}$$

Summing over ε_n in Eqs. (38) and (39), one finally obtains

$$\Delta_{1\mathrm{ph}} = -\frac{4g_1}{(\hbar\omega_{0(1)} - 2zV_a)} \times \frac{\varepsilon - 2g_1\Delta_{1\mathrm{ph}}}{2s}\tanh\left(\frac{s}{2k_BT}\right), \tag{40}$$

$$\Delta_{2\mathrm{ph}} = \frac{4g_2}{(\hbar\omega_{0(2)} - 2zV_b)}\frac{\left(zJ_{\mathrm{ex}}\Delta_{\mathrm{ex}} + g_2\Delta_{2\mathrm{ph}}\right)}{s}\tanh\left(\frac{s}{2k_BT}\right). \tag{41}$$

The expressions for the phonon order parameters given above are valid in the limit when $g_1 << \omega_{0(1)}$ and $g_2 << \omega_{0(2)}$.

Using the expression

$$\left\langle c^{\dagger}_{\lambda' g\gamma}c_{\lambda f\gamma}\right\rangle = -\frac{1}{\pi}\int d\omega f_F(\omega,\mu)\mathrm{Im}G^{\gamma}_{\lambda\lambda'}(f-g,\omega+i\delta)$$

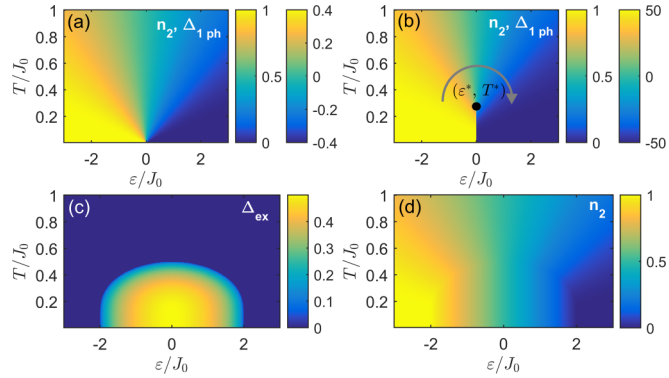

FIG. 6. The mean-field phase diagrams in the following cases: (a) $g_1 = 0.01J_0$, $J''_{\mathrm{ex}} = 0$, $V_a = 0$; (b) $g_1 = 0.01J_0$, $J''_{\mathrm{ex}} = 0$, $V_a = 0.0124J_0$, (c) and (d) $J''_{\mathrm{ex}} = -0.5J_0$, $V_a = 0$, $g_1 = 0$. In (a) and (b), the first color scale corresponds to n_2, the second corresponds to $\Delta_{1\mathrm{ph}}$, (ε^*_S, T^*) is the critical vapor-liquid point.

for the correlation function together with Eq. (36), the occupation numbers of the states 1 and 2 are

$$n_1 = \frac{1}{2}\left[1 + \frac{\varepsilon/2 - g_1\langle a_i + a_i^{\dagger}\rangle}{s}\tanh\left(\frac{s}{2k_BT}\right)\right], \tag{42}$$

$$n_2 = \frac{1}{2}\left[1 - \frac{\varepsilon/2 - g_1\langle a_i + a_i^{\dagger}\rangle}{s}\tanh\left(\frac{s}{2k_BT}\right)\right], \tag{43}$$

and the excitonic order parameter is

$$\Delta_{\mathrm{ex}} = -\frac{zJ_{\mathrm{ex}}\Delta_{\mathrm{ex}} + g_2\Delta_{2\mathrm{ph}}}{2s}\tanh\left(\frac{s}{2k_BT}\right). \tag{44}$$

Among the solutions of Eqs. (40)–(44) we are interested in those which correspond to the free energy $F = -k_BT\ln(e^{-\beta\omega_1} + e^{\beta\omega_1})$ minimum and satisfy the equation, defining the value of the chemical potential

$$n_1 + n_2 = 1 = -\frac{1}{\pi}\int d\omega f_F(\omega,\mu)\left[\mathrm{Im}G^{\gamma}_{11}(\omega+i\delta) + \mathrm{Im}G^{\gamma}_{22}(\omega+i\delta)\right].$$

Let us investigate the roles of various interactions in Eq. (33). As in Sec. IV, we consider the case of a two-dimensional square lattice and neglect J'_{ex}. The frequencies $\omega_{0(1)}$ and $\omega_{0(2)}$ in Eqs. (34) and (35) are supposed to be equal to $0.1J_0$. To simplify the discussion we will also assume that $V_b = 0$ (an influence of this parameter will be discussed below).

First, we consider the case $g_2 = 0$. In Figs. 6(a) and 6(b) the phase diagrams of the phonon order parameter $\Delta_{1\mathrm{ph}}$ [Eq. (40)] and the occupation number n_2 [Eq. (43)] are shown at $J''_{\mathrm{ex}} = 0$, $g_1 = 0.01J_0$ in the case when $V_a = 0$ (a) and $V_a = 0.0124J_0$ (b). In the first case (a) there is a smooth crossover, whereas in the second (b) there is an isostructural first order phase transition with the critical "vapor-liquid" point (ε^*, T^*) present—above this point, the system can be smoothly transformed from a state with $n_2 = 1$ to a state with $n_2 = 0$. The case $V_a \neq 0$ and $g_1 = 0$ is trivial, since, according to Eq. (40), $\Delta_{1\mathrm{ph}} = 0$, and the Hamiltonian Eq. (34) can be diagonalized by a canon-

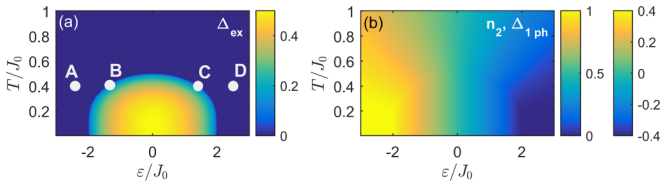

FIG. 7. The phase diagrams of (a) the excitonic order parameter Δ_{ex}, (b) the occupation number n_2 of the one-electron state 2 and the phonon order parameter Δ_{1ph} at $g_2 = 0$ and $V_a = 0$. In (b), the first color scale corresponds to n_2, the second corresponds to Δ_{1ph}

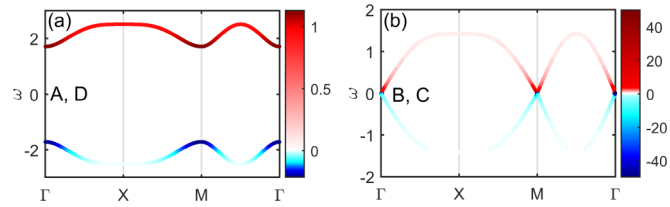

FIG. 8. The spectrum of excitons $\omega_{\pm}(\mathbf{k})$ given by Eq. (46) calculated at the points A, B, C, and D of the phase diagram Fig. 7(a) when $g_2 = 0$.

ical transformation as $H_{1ph} = \sum_{\mathbf{q}} \omega(\mathbf{q})(a^{\dagger}_{\mathbf{q}} a_{\mathbf{q}} + 1/2)$, where $\omega(\mathbf{q}) = \hbar\omega_{0(1)}\sqrt{(1 - \frac{4V_a}{\hbar\omega_{0(1)}}(\cos q_x + \cos q_y))}$, which describes an ideal gas of phonons, in which, as in Fig. 6, there is no phase transition. Comparing Figs. 6(a) and 6(b), it can be seen that the intersite interaction V_a provides the cooperativity necessary for a phase transition. Each of the interactions V_a and g_1 separately does not lead to a phase transition (the presence of one of them separately is necessary, but not sufficient). In the following we will exclude the phonon mechanism of cooperativity by assuming $V_a = 0$.

Whereas the phase diagram shown in Fig. 6(a) corresponds to the quantum phase transition at $T = 0$ in the absence of cooperativity, in Fig. 6(b) there is a first order phase transition at finite temperatures up to the critical point T^*. In Figs. 6(c) and 6(d) the phase diagram of the excitonic order parameter Δ_{ex} given by Eq. (44) and the phase diagram of the occupation number n_2 given by Eq. (43) are shown at $J''_{ex} = -0.5J_0$ when $V_a = 0$ and $g_1 = 0$. In such a case there exists the second order phase transition into the excitonic condensate phase [see Fig. 6(c)].

The results of calculations in the case when Δ_{ex}, n_2, and Δ_{1ph} are nonzero at the same time, but V_a is zero, are shown in Figs. 7(a) and 7(b) at $J''_{ex} = -0.5J_0$ and $g_1 = 0.01J_0$. From Figs. 6(a), 6(b) and 7(b) it is clear that n_2 and Δ_{1ph} behave similarly [see Eqs. (40) and (43)].

Analogously to Eq. (20) one obtains the two-electron Green function

$$\langle\langle c^{\dagger}_{1f\gamma} c_{2f\gamma} | c^{\dagger}_{2g\gamma} c_{1g\gamma} \rangle\rangle = \frac{(n_1 - n_2)}{(\omega - \omega_+)(\omega - \omega_-)}[\omega + \varepsilon - 2g_1 \times \Delta_{1ph} + (n_1 - n_2)J'_{ex}(\mathbf{k})], \quad (45)$$

$$\omega_{\pm}(\mathbf{k}) = \pm\,[(\varepsilon - 2g_1\Delta_{1ph} + (n_1 - n_2)J'_{ex}(\mathbf{k}))^2 - (n_1 - n_2)^2 J''^2_{ex}(\mathbf{k})]^{1/2}. \quad (46)$$

The spectrum of excitons given by Eq. (46) at the points A, B, C, and D of the phase diagram Fig. 7(a) is shown in Fig. 8. We define the excitonic spectrum gap as $E_g = \omega_+(\mathbf{k}) - \omega_-(\mathbf{k})$, where $\mathbf{k} = \Gamma(M)$. The diagonal electron-phonon interaction does not lower the symmetry of the Hamiltonian in Eq. (32), so the gap E_g is zero at the boundary of the excitonic condensate phase (see Fig. 8, B and C).

Let us now discuss the case $g_1 = 0$, but $g_2 = 0.01J_0$ ($J''_{ex} = -0.5J_0$ as before) shown in Fig. 9. Due to Eq. (44) the behavior of Δ_{ex} and Δ_{2ph} is qualitatively identical. In this case, the nondiagonal electron-phonon interaction lowers the symmetry of the Hamiltonian in Eq. (32), thus, the gap E_g is finite and remains open at the excitonic condensate boundary (see Fig. 10, points B and C).

As one can see from Figs. 8 and 10 (similarly to Figs. 3–5), the spectral weight is distributed nonuniformly among the Brillouin zone. We note that since at $\varepsilon = 0$ a change of the ground state takes place, the system cannot be smoothly (adiabatically) transformed from the state at point A to the state at point D. This way, across the line $\varepsilon = 0$, as one can see from Eq. (46) ($n_1 = n_2 = 0.5$ at $\varepsilon = 0$), the gap becomes zero even when the nondiagonal electron-phonon interaction is present.

VI. DISCUSSION AND CONCLUSIONS

Using Eq. (1), one can consider two limiting cases. In the first (weakly correlated), when $H_{\text{Coulomb}} << H_{\Delta} + H_t$, one deals with a two-band semiconductor or a semimetal, depending on the t/Δ ratio. In this case, the Bose-Einstein or BCS formation of excitonic condensate is possible. In the second case (strongly correlated), when the energy of the Coulomb interaction of electrons is comparable to the crystal field energy $H_{\text{Coulomb}} \sim H_{\Delta}$ and larger than their kinetic energy $H_{\text{Coulomb}} > H_t$, there appears a possibility for the spin crossover and formation of localized magnetic excitons. In the present paper we have shown in the framework of the two-band Hubbard-Kanamori model that the condensation of such excitons takes place near the spin crossover and leads to the appearance of the antiferromagnetic ordering even when an interatomic exchange interaction is absent. In other words, the appearance of magnetism caused by excitonic condensation is found. It should be noted that in the exciton dielectric model at weak electron-electron interaction, the formation of excitonic condensate can lead to magnetic ordering without exchange interaction in a similar way [4].

Close to the phase transition point the elementary excitation spectra are known for their significant dependency on the type of statistics: whereas in the fermion system, a gapped branch with a gap width proportional to the order parameter

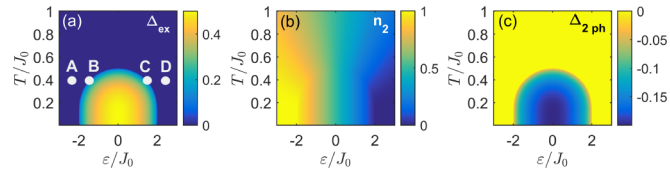

FIG. 9. The phase diagrams of the (a) excitonic order parameter Δ_{ex}, (b) occupancy n_2, and (c) phonon order parameter Δ_{2ph} in the case $g_1 = 0$.

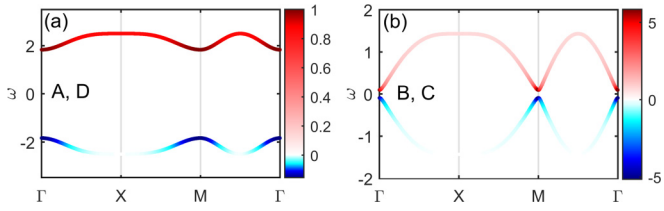

FIG. 10. The spectrum of excitons $\omega_{\pm}(\mathbf{k})$ given by Eq. (46) calculated at the points A, B, C, and D of Fig. 9(a) when $g_2 \neq 0$.

exists as well as a gapless branch, in the Bose system only the latter exists. This is due to the fact that fermionic systems have both individual gapped and collective gapless excitations, while Bose systems can only have collective excitations (as was shown using the diagrammatic approach in Ref. [39]).

In the present paper we have obtained the spectrum of exciton excitations and shown its instability towards the formation of the excitonic Bose condensate. This spectrum describes collective, from the point of view of the electronic (Fermi) system, excitations, but one can interpret this spectrum as a quasiparticle (one-particle) one with respect to Bose-type particles described by the Hamiltonian in Eq. (15). Everywhere outside the excitonic condensate phase there is a gap in the spectrum, which becomes zero at the boundary of the second order phase transition, which agrees with the general idea, that, below the point of a phase transition, there should arise a gapless Goldstone mode, describing collective excitations in the excitonic condensate phase [16,40]. In other words, the appearance of such a gapless mode is preceded by the closing of the gap in the quasiparticle excitations spectrum. The nondiagonal electron-phonon interaction (contrary to the diagonal one) leads to the opening of a gap in the individual excitonic excitations spectrum at the boundary of the second order phase transition, which is consistent with the result of Ref. [40], where it was shown that the collective Goldstone mode acquires mass due to nondiagonal electron-phonon interaction. In this case, the Bose spectrum of excitations (one-particle excitonic and collective in the excitonic phase) has a gap on both sides of the phase transition. According to the authors of Ref. [40], this circumstance plays an important role in the photoinduction of an excitonic condensate and can provide a new strategy of enhancing the order parameter in analogous systems (such as superconductors). An interesting feature of the spectra that we obtained is the nonuniform spectral weight distribution among the Brillouin zone. In this connection, it is interesting to investigate the behavior of collective excitations in the exciton condensate phase.

Let us discuss the possibility of experimental realization of our results. As was mentioned in the Introduction, $LaCoO_3$ and other rare earth cobaltites with competition between magnetic and nonmagnetic terms can be described by our model, see also the review [15] and papers [16–21]. In $LaCoO_3$, continuous occupation of the magnetic term with heating prevents a thermodynamic phase transition. Another external force that may induce spin crossover in $LaCoO_3$ is a strong magnetic field. Several experiments have confirmed the LS-HS state transition in magnetic field 65 T [41–44]. Field-induced exciton condensation in $LaCoO_3$ has been discussed in papers [45–47].

The crossover between magnetic HS and nonmagnetic LS states under high pressure in ferropericlase $Fe_xMg_{1-x}O$ was mentioned in the Introduction. In the limit $T \to 0$ the crossover becomes a quantum phase transition of a pure topological nature and emerges as the quantum transition between the ground states with the distinct winding numbers [48,49]. To check the prediction [29] that spin crossover at zero temperature is a quantum phase transition with topological Berry-type phase as the order parameter, the detailed study of nuclear forward scattering at pressures up to 60 GPa and temperature between 8 and 300 K have been carried out [50]. The finite temperature is expected to smooth the quantum phase transition. What was found in experiment [50] is the first order transition from magnetic HS state to nonmagnetic LS state as the vertical line on a (P, T) plane with $P_c = 55$ GPa. The excitonic phase may be expected at low temperatures at pressure around 55 GPa.

Another possible experiment related to our conclusions is a study of the excitonic dispersion even far from spin crossover. It may be done both in $LaCoO_3$ and under high pressure in ferropericlase $Fe_xMg_{1-x}O$. Inelastic neutron scattering experiments had shown its capabilities to measure dispersion of various boson-type excitations like phonons, magnons, etc. For experiments under high pressure RIXS might be more available.

ACKNOWLEDGMENT

The authors thank the Russian Scientific Foundation for financial support under Grant No. 18-12-00022.

[1] N. F. Mott, Philos. Mag. **6**, 287 (1961).
[2] R. S. Knox, *Solid State Phys. Suppl. 5* (Academic Press, 1963).
[3] L. V. Keldysh and Y. V. Kopaev, Soviet Phys. Solid State **6**, 2219 (1965).
[4] B. A. Volkov, Y. V. Kopaev, and A. I. Rusinov, Sov. Phys. JETP **41**, 952 (1975).
[5] M. Matsumoto, B. Normand, T. M. Rice, and M. Sigrist, Phys. Rev. B **69**, 054423 (2004).
[6] T. Giamarchi, C. Rüegg, and O. Tchernyshyov, Nat. Phys. **4**, 198 (2008).
[7] S. Sachdev and B. Keimer, Phys. Today **64**, 29 (2011).
[8] Y. Kulik and O. P. Sushkov, Phys. Rev. B **84**, 134418 (2011).
[9] T. Sommer, M. Vojta, and K. W. Becker, Eur. Phys. J. B **23**, 329 (2001).
[10] R. Shiina, J. Phys. Soc. Jpn. **73**, 2257 (2004).
[11] J. c. v. Chaloupka and G. Khaliullin, Phys. Rev. Lett. **110**, 207205 (2013).
[12] G. Khaliullin, Phys. Rev. Lett. **111**, 197201 (2013).
[13] A. Jain, M. Krautloher, J. Porras, G. Ryu, D. Chen, D. Abernathy, J. Park, A. Ivanov, J. Chaloupka, G. Khaliullin *et al.*, Nat. Phys. **13**, 633 (2017).
[14] S.-M. Souliou, J. c. v. Chaloupka, G. Khaliullin, G. Ryu, A. Jain, B. J. Kim, M. Le Tacon, and B. Keimer, Phys. Rev. Lett. **119**, 067201 (2017).
[15] J. Kuneš, J. Phys.: Condens. Matter **27**, 333201 (2015).

[16] J. Nasu, T. Watanabe, M. Naka, and S. Ishihara, Phys. Rev. B **93**, 205136 (2016).
[17] P. Werner and A. J. Millis, Phys. Rev. Lett. **99**, 126405 (2007).
[18] R. Suzuki, T. Watanabe, and S. Ishihara, Phys. Rev. B **80**, 054410 (2009).
[19] L. Balents, Phys. Rev. B **62**, 2346 (2000).
[20] T. Kaneko and Y. Ohta, Phys. Rev. B **90**, 245144 (2014).
[21] J. Kuneš and P. Augustinský, Phys. Rev. B **89**, 115134 (2014).
[22] I. S. Lyubutin and A. G. Gavriliuk, Phys. Usp. **52**, 989 (2009).
[23] W. Xu, W. Dong, S. Layek, M. Shulman, K. Glazyrin, E. Bykova, M. Bykov, M. Hanfland, M. P. Pasternak, I. Leonov *et al.*, Sci. Rep. **12**, 9647 (2022).
[24] J. Badro, G. Fiquet, F. Guyot, J.-P. Rueff, V. V. Struzhkin, G. Vanko, and G. Monaco, Science **300**, 789 (2003).
[25] J.-F. Lin, A. G. Gavriliuk, V. V. Struzhkin, S. D. Jacobsen, W. Sturhahn, M. Y. Hu, P. Chow, and C.-S. Yoo, Phys. Rev. B **73**, 113107 (2006).
[26] I. Y. Kantor, L. S. Dubrovinsky, and C. A. McCammon, Phys. Rev. B **73**, 100101(R) (2006).
[27] A. G. Gavriliuk, J. Lin, I. S. Lyubutin, and V. Struzhkin, JETP Lett. **84**, 161 (2006).
[28] Y. S. Orlov, S. V. Nikolaev, V. A. Dudnikov, and S. G. Ovchinnikov, Phys. Rev. B **104**, 195103 (2021).
[29] A. Nesterov and S. G. Ovchinnikov, JETP Lett. **90**, 530 (2009).
[30] Y. S. Orlov, S. V. Nikolaev, and V. A. Dudnikov, J. Exp. Theor. Phys. **130**, 699 (2020).
[31] J. Kanamori, Prog. Theor. Phys. **30**, 275 (1963).
[32] J. Hubbard, Proc. R. Soc. London Ser. A **277**, 237 (1964).
[33] R. O. Zaitsev, Sov. Phys. JETP **43**, 574 (1976).
[34] K. A. Chao, J. Spalek, and A. M. Oles, J. Phys. C **10**, L271 (1977).
[35] V. A. Gavrichkov, S. I. Polukeev, and S. G. Ovchinnikov, Phys. Rev. B **95**, 144424 (2017).
[36] V. V. Val'kov and S. G. Ovchinnikov, Theor. Math. Phys. **50**, 306 (1982).
[37] S. V. Vonsovskii and M. S. Svirskii, Sov. Phys. JETP **20**, 914 (1965).
[38] M. J. R. Hoch, S. Nellutla, J. van Tol, E. S. Choi, J. Lu, H. Zheng, and J. F. Mitchell, Phys. Rev. B **79**, 214421 (2009).
[39] A. A. Migdal, Sov. Phys. JETP **28**, 1036 (1969).
[40] Y. Murakami, D. Golež, M. Eckstein, and P. Werner, Phys. Rev. Lett. **119**, 247601 (2017).
[41] A. Ikeda, T. Nomura, Y. H. Matsuda, A. Matsuo, K. Kindo, and K. Sato, Phys. Rev. B **93**, 220401(R) (2016).
[42] V. Platonov, Y. B. Kudasov, M. Monakhov, and O. Tatsenko, Phys. Solid State **54**, 279 (2012).
[43] M. M. Altarawneh, G.-W. Chern, N. Harrison, C. D. Batista, A. Uchida, M. Jaime, D. G. Rickel, S. A. Crooker, C. H. Mielke, J. B. Betts, J. F. Mitchell, and M. J. R. Hoch, Phys. Rev. Lett. **109**, 037201 (2012).
[44] M. Rotter, Z.-S. Wang, A. Boothroyd, D. Prabhakaran, A. Tanaka, and M. Doerr, Sci. Rep. **4**, 7003 (2014).
[45] A. Sotnikov and J. Kuneš, Sci. Rep. **6**, 30510 (2016).
[46] T. Tatsuno, E. Mizoguchi, J. Nasu, M. Naka, and S. Ishihara, J. Phys. Soc. Jpn. **85**, 083706 (2016).
[47] A. Ikeda, S. Lee, T. T. Terashima, Y. H. Matsuda, M. Tokunaga, and T. Naito, Phys. Rev. B **94**, 115129 (2016).
[48] G. E. Volovik, *The Universe in a Helium Droplet* (Oxford University Press, Oxford, 2003), Vol. 117.
[49] G. E. Volovik, Quantum phase transitions from topology in momentum space, in *Quantum Analogues: From Phase Transitions to Black Holes and Cosmology*, edited by W. G. Unruh and R. Schützhold (Springer, Berlin, 2007), pp. 31–73.
[50] I. S. Lyubutin, V. V. Struzhkin, A. A. Mironovich, A. G. Gavriliuk, P. G. Naumov, J.-F. Lin, S. G. Ovchinnikov, S. Sinogeikin, P. Chow, Y. Xiao, and R. J. Hemley, Proc. Natl. Acad. Sci. **110**, 7142 (2013).